

# Ultra-Broadband Passive Phase Shifter Using Anisotropic Subwavelength Metamaterials

David González-Andrade<sup>1,\*</sup>, José Manuel Luque-González<sup>2</sup>, J. Gonzalo Wangüemert-Pérez<sup>2</sup>, Alejandro Ortega-Moñux<sup>2</sup>, Pavel Cheben<sup>3</sup>, Íñigo Molina-Fernández<sup>2,4</sup>, Aitor V. Velasco<sup>1</sup>

<sup>1</sup> Instituto de Óptica Daza de Valdés, Consejo Superior de Investigaciones Científicas (CSIC), Madrid 28006, Spain

<sup>2</sup> Departamento de Ingeniería de Comunicaciones, ETSI Telecomunicación, Universidad de Málaga, Málaga 29071, Spain

<sup>3</sup> National Research Council Canada, 1200 Montreal Road, Bldg. M50, Ottawa K1A 0R6, Canada

<sup>4</sup> Bionand Center for Nanomedicine and Biotechnology, Parque Tecnológico de Andalucía, Málaga 29590, Spain  
e-mail: [david.gonzalez@csic.es](mailto:david.gonzalez@csic.es)

## ABSTRACT

Optical phase shifters are a cornerstone constituent in most photonic integrated circuits aimed at high-end applications. However, most progress has focused on active phase shifters in recent years, while passive phase shifters have barely evolved. Here, we propose a new type of ultra-broadband passive phase shifter that exploits anisotropy and dispersion engineering in subwavelength metamaterial waveguides. Floquet-Bloch simulations of our proposed device predict a phase shift error below  $\pm 1.7^\circ$  over an outstanding 400 nm bandwidth (1.35 – 1.75  $\mu\text{m}$ ). The subwavelength engineered PS was fabricated on an SOI platform and our measurements show a four-fold reduction in the phase variation compared to other conventional phase shifters based on tapered waveguides.

**Keywords:** phase shifter, silicon-on-insulator, subwavelength grating, metamaterial, ultra-broadband.

## 1. INTRODUCTION

Silicon-on-insulator (SOI) has become a ubiquitous platform for the development of several cutting-edge applications, including telecom and datacom, sensing, quantum computing, and microwave and terahertz photonics [1]-[3], to name a few. The SOI platform benefits from the compatibility with already-existing CMOS facilities that enables mass production of photonic integrated circuits (PICs) in a cost-effective way. Additionally, the high refractive index contrast between the silicon core waveguide and the silicon dioxide ( $\text{SiO}_2$ ) layer results in a dense integration of photonic devices on a single chip, which facilitates the miniaturization of complex photonic systems.

Most PICs rely on fundamental building blocks like beam splitters [4], filters [5] and (de)multiplexers [6]. Optical phase shifters (PSs) are another essential constituent in photonic systems to induce a specific phase shift between different signals. In the last years, research efforts have mainly focused on the development of active phase shifters (PSs), especially for the implementation of optical modulators and switches. These devices are typically based on thermo-optic [7] or free carrier plasma dispersion [8] effects that enable to dynamically tune the phase shift between signals by means of an active control element. Conversely, passive PSs have barely evolved and are usually replaced by active PSs to compensate for possible fabrication errors or to adjust the phase response at a particular wavelength. However, passive PSs are attracting increasing attention for a wide range of applications such as mode-division multiplexing (MDM), optical 90° hybrids, beam splitting for different mode orders and for arbitrary power ratios [9]-[11].

In this work, we present an ultra-broadband passive 90° PS exploiting dispersion and anisotropy engineering in subwavelength grating (SWG) metamaterial waveguides. Our Floquet-Bloch simulations predict a phase error as low as  $\pm 1.7^\circ$  over an outstanding 400 nm bandwidth (1.35 – 1.75  $\mu\text{m}$ ) for transverse electric (TE) polarization. The device was fabricated and a phase slope of only  $16^\circ/\mu\text{m}$  was measured within a 145 nm wavelength range (1.495 – 1.64  $\mu\text{m}$ ), limited by the laser source of our setup. This is a remarkable four-fold reduction compared to the  $64^\circ/\mu\text{m}$  measured for a conventional PS based on tapered waveguides.

## 2. DESIGN

The proposed PS is based on two parallel SWG waveguides of the same length as schematically shown in Fig. 1(a). SWG structures are an alternating disposition of different materials with a pitch below half the wavelength, which behave as a diffraction-less anisotropic medium [12]. For the design, we considered an SOI material platform based on 220-nm-thick Si waveguides and  $\text{SiO}_2$  buried oxide (BOX) and upper cladding layers. The width of both waveguides must be wide enough to hold paraxiality condition [13] and, at the same time, to improve tolerances to width deviations, i.e. the variation of the effective index with respect to changes in width is lower than for narrow waveguides. In this way, the phase shift induced between two wide SWG waveguides can be simplified to [14]:

$$\Delta\Phi(\lambda) \approx \frac{\pi\lambda n_{xx}}{4n_{zz}^2} \left( \frac{1}{W_{e,B}^2} - \frac{1}{W_{e,A}^2} \right) L_{PS}, \quad (1)$$

where  $\lambda$  is the free-space wavelength,  $W_e$  is the effective width,  $L_{PS}$  is the length of the SWG waveguides, and  $n_{xx}$  and  $n_{zz}$  are the refractive indexes of the 2D equivalent anisotropic medium in the  $x$  and  $z$  directions, respectively.

By judiciously selecting the pitch ( $\Lambda$ ) and the duty cycle (DC) of the SWG waveguides, the term  $n_{xx}/n_{zz}^2$  can be engineered to be inversely proportional to  $\lambda$ , thus yielding an almost flat phase shift response. To this end, we selected widths of  $W_A = 1.8 \mu\text{m}$  and  $W_B = 1.6 \mu\text{m}$ , a pitch value of 200 nm and a duty cycle of 50% to ensure a minimum feature size of 100 nm. Moreover, SWG tapers of  $L_T = 3 \mu\text{m}$  were included to perform an adiabatic transition between the non-periodic waveguides ( $W_I = 500 \text{ nm}$ ) and wide SWG waveguides. Taking into account that the phase shift introduced by SWG tapers is approximately  $20^\circ$ , the length of the phase shifting section is only  $L_{PS} = 16.8 \mu\text{m}$  to achieve a total  $90^\circ$  phase shift at the design wavelength of  $1.55 \mu\text{m}$ .

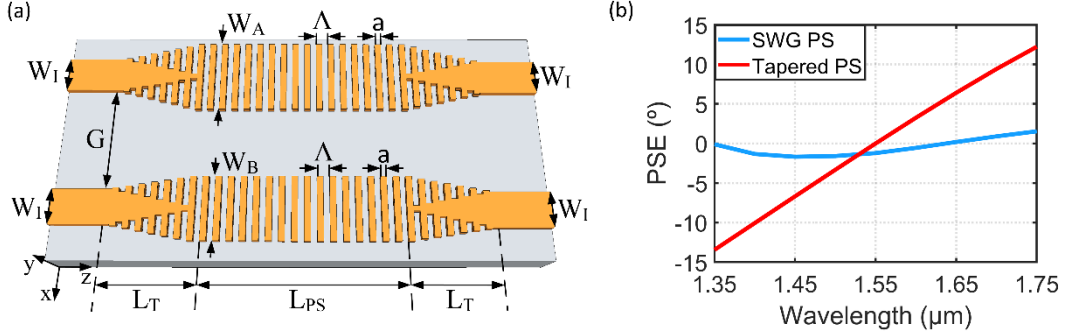


Figure 1. (a) Schematic of the proposed phase shifter based on SWG metamaterial waveguides. (b) Simulated phase shift error as a function of the wavelength for the SWG PS (blue curve) compared to a conventional PS based on two tapers in back-to-back configuration and a straight waveguide (red curve).

To assess the performance of the designed  $90^\circ$  PSs, we define the phase shift error (PSE) as the deviation from the target  $90^\circ$  phase shift. Figure 1(b) shows the PSE as a function of the wavelength for our SWG PS (represented with the blue curve) and a conventional PS based on two tapers in back-to-back configuration and a straight waveguide (in red). It should be noted that the tapered PS is also designed to perform a  $90^\circ$  phase shift. A small PSE of only  $\pm 1.7^\circ$  is attained for the proposed SWG PS over an ultra-broad bandwidth of 400 nm ( $1.35 - 1.75 \mu\text{m}$ ), whereas the conventional PS yields a PSE of  $\pm 13.5^\circ$  within the same wavelength range.

### 3. EXPERIMENTAL RESULTS

Both SWG and tapered PSs were fabricated on a 220-nm-thick SOI platform with 2- $\mu\text{m}$ -thick BOX using electron beam (e-beam) lithography and a reactive ion etching (RIE) process. Scanning electron microscope (SEM) of the fabricated devices are shown in Figs. 2(a) and 2(b), respectively. After taking SEM images, the circuit was covered with a 2.2- $\mu\text{m}$ -thick  $\text{SiO}_2$  upper cladding.

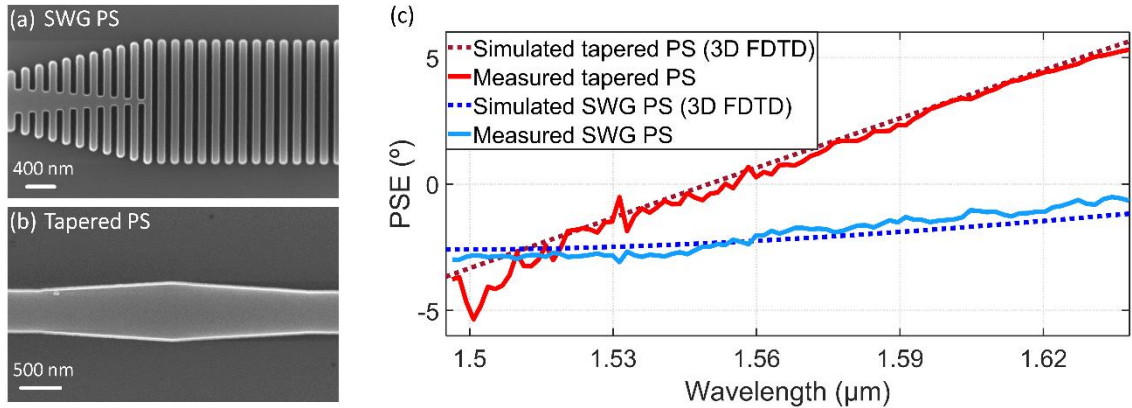


Figure 2. Scanning electron microscope images of the upper arm of (a) our proposed SWG PS and (b) the tapered PS. (c) Measured phase shift error as a function of the wavelength for the SWG PS (blue) and the tapered PS (red). 3D FDTD simulation results are included (dotted lines) for comparison.

To experimentally characterize the fabricated PSs, we used Mach-Zehnder interferometer (MZI) consisting of two SWG multimode interference (MMI) couplers and 14 PSs connected in series. The intensity signal measured at the MZI output is modulated with a period depending on the optical path delay between the arms of the MZI,

i.e. based on the phase shift response of the PSs. We developed a circuit model to simulate the MZI and estimate the phase error introduced by fabrication deviations. These errors were subtracted from the measured phase shift response, which was obtained by solving the matrix system posed by the MZI test structure when transmission matrices are considered [14].

Figure 2(c) shows that the measured wavelength dependence of tapered and SWG PSs (solid curves) are in very good agreement with our 3D finite difference time domain (FDTD) simulation results (dotted curves). The proposed SWG PS provides a phase slope as small as  $16^\circ/\mu\text{m}$ , whereas the tapered PS based on conventional (non-periodic) waveguides yields a phase slope of  $64^\circ/\mu\text{m}$ . This is a four-fold enhancement in terms of bandwidth within the measured wavelength range of 145 nm ( $1.495 - 1.64 \mu\text{m}$ ).

#### 4. CONCLUSIONS

In conclusion, we report on the experimental demonstration of an ultra-broadband PS based on waveguides of equal length. Limitations posed by conventional PSs based on non-periodic waveguides are overcome by exploiting the additional degrees of freedom provided by SWG metamaterial waveguides. Our proposed SWG PS leverages inherent anisotropy properties of SWG waveguides in combination with dispersion engineering to achieve a simulated phase shift error of only  $\pm 1.7^\circ$  over an unprecedented 400 nm bandwidth. The device was fabricated and the concept of flattening the phase response was verified, showing a four-fold reduction compared to the tapered PS over the measured 145 nm bandwidth ( $1.495 - 1.64 \mu\text{m}$ ). The proposed SWG PS opens new venues for the implementation of PICs targeting cutting-edge applications like quantum photonics and MDM.

#### ACKNOWLEDGEMENTS

This work has been funded in part by the Spanish Ministry of Science, Innovation and Universities (MICINN) under grants RTI2018-097957-B-C33, TEC2015-71127-C2-1-R (FPI BES-2016-077798), CDTI SNEO-20181232 (Alcyon Photonics S.L.), and TEC2016-80718-R; the Spanish Ministry of Education, Culture and Sport (MECD) (FPU16/06762); and the Community of Madrid – FEDER funds (S2018/NMT-4326). This project has received funding from the Horizon 2020 research and innovation program under the Marie Skłodowska-Curie No. 734331.

#### REFERENCES

- [1] J. G. Wangüemert-Pérez, *et al.*: Subwavelength structures for silicon photonics biosensing, *Opt. Laser Technol.*, vol. 109. pp. 437-448, Jan. 2019.
- [2] N. C. Harris, *et al.*: Large-scale quantum photonic circuits in silicon, *Nanophotonics*, vol. 5. pp. 456-468, March 2016.
- [3] D. Marpaung, *et al.*: Integrated microwave photonics, *Nat. Photonics*, vol. 13. pp. 80-90, Jan. 2019.
- [4] D. González-Andrade, *et al.*: Polarization- and wavelength-agnostic nanophotonic beam splitter, *Sci. Rep.*, vol. 9. pp. 3604, Mar. 2019.
- [5] D. Oser, *et al.*: Coherency-broken Bragg filters: overcoming on-chip rejection limitations, *Laser Photon. Rev.*, vol. 13. pp. 1800226, Jul. 2019.
- [6] P. J. Bock, *et al.*: Demonstration of a curved sidewall grating demultiplexer on silicon, *Opt. Express*, vol. 20. pp. 19882-19892, Aug. 2012.
- [7] G. Cocorullo, *et al.*: Temperature dependence of the thermo-optic coefficient in crystalline silicon between room temperature and 550 K at the wavelength of 1523 nm, *Appl. Phys. Lett.*, vol. 74. pp. 3338-3340, Apr. 1999.
- [8] R. A. Soref, *et al.*: Electrooptical effects in silicon, *IEEE J. Quantum Electron.*, vol. 23. pp. 123-129, Jan. 1987.
- [9] D. González-Andrade, *et al.*: Ultra-broadband mode converter and multiplexer based on sub-wavelength structures, *IEEE Photonics J.*, vol. 10. pp. 2201010, Apr. 2018.
- [10] M. Cherchi, *et al.*: Unconstrained splitting ratios in compact double-MMI couplers, *Opt. Express*, vol. 22. pp. 9245-9253, Apr. 2014.
- [11] F. Ren, *et al.*: Variable-ratio mode-insensitive  $1 \times 2$  power splitter based on MMI couplers and phase shifters, *IEEE Photonics J.*, vol. 10. pp. 7104912, Sep. 2018.
- [12] P. Cheben, *et al.*: Subwavelength integrated photonics, *Nature*, vol. 560. pp. 565-572, Aug. 2018.
- [13] L. B. Soldano, *et al.*: Optical multi-mode interference devices based on self-imaging: principles and applications, *J. Lightwave Technol.*, vol. 13. pp. 615-627, Apr. 1995.
- [14] D. González-Andrade, *et al.*: Ultra-broadband nanophotonic phase shifter based on subwavelength metamaterial waveguides, *Photon. Res.*, doc. ID 373223 (posted 24 December 2019, in press).